

# Thermal neutron induced (n,p) and (n, $\alpha$ ) reactions on $^{37}\text{Ar}$

R. Bieber<sup>a,1</sup>, C. Wagemans<sup>b</sup>, G. Goeminne<sup>b</sup>, J. Wagemans<sup>a</sup>, B. Denecke<sup>a</sup>,  
M. Loiselet<sup>c</sup>, M. Gaelens<sup>c</sup>, P. Geltenbort<sup>d</sup> and H. Oberhummer<sup>e</sup>

<sup>a</sup> EC, JRC, Institute for Reference Materials and Measurements, Retieseweg, B-2440 Geel, Belgium

<sup>b</sup> Dept. of Subatomic and Radiation Physics, RUG, Proeftuinstraat 86, B-9000 Gent, Belgium

<sup>c</sup> Cyclotron Research Center, UCL, Chemin du Cyclotron 2, B-1348 Louvain-la-Neuve, Belgium

<sup>d</sup> Institute Laue-Langevin, B.P.156, F-38042 Grenoble, France

<sup>e</sup> University of Technology Vienna, Wiedner Hauptstr. 8-10, A-1040 Vienna, Austria

**Abstract:** The  $^{37}\text{Ar}(n_{\text{th}},\alpha)^{34}\text{S}$  and  $^{37}\text{Ar}(n_{\text{th}},p)^{37}\text{Cl}$  reactions were studied at the high flux reactor of the ILL in Grenoble. For the  $^{37}\text{Ar}(n_{\text{th}},\alpha_0)^{34}\text{S}$  and  $^{37}\text{Ar}(n_{\text{th}},p)^{37}\text{Cl}$  reaction cross sections, values of  $(1070 \pm 80)$  b and  $(37 \pm 4)$  b, respectively, were obtained. Both values are about a factor 2 smaller than results of older measurements. The observed suppression of the  $^{37}\text{Ar}(n_{\text{th}},\alpha_1)^{34}\text{S}$  transition could be verified from theoretical considerations. Finally, evidence was found for the two-step  $^{37}\text{Ar}(n_{\text{th}},\gamma\alpha)^{34}\text{S}$  process.

**Keywords:**

NUCLEAR REACTIONS  $^{37}\text{Ar}(n_{\text{th}},\alpha)^{34}\text{S}$ ,  $^{37}\text{Ar}(n_{\text{th}},\gamma\alpha)^{34}\text{S}$ ,  $^{37}\text{Ar}(n_{\text{th}},p)^{37}\text{Cl}$ ; thermal neutron energy; measured alpha and proton yields; deduced reaction cross section; calculated  $(n_{\text{th}},\alpha_0)/(n_{\text{th}},\alpha_1)$  branching ratio. PACS: 25.40.-h, 26.30.+k, 26.45.+h, 27.30.+t

<sup>1</sup> present address: Kernfysisch Versneller Instituut, Rijksuniversiteit Groningen, Zernikelaan 25, NL-9744 AA Groningen, The Netherlands

## 1 Introduction

One of the few nuclides with fairly large positive reaction energies for both proton and alpha emission after thermal neutron capture is  $^{37}\text{Ar}$ . The large  $Q_\alpha$ -values for the transitions to the ground and first excited state of  $^{34}\text{S}$  and the gap of about 2 MeV between them makes it also a good candidate for the study of the two-step  $(n_{\text{th}}, \gamma\alpha)$  decay.

From an astrophysical point of view, the  $^{37}\text{Ar}(n, \alpha)^{34}\text{S}$  and  $^{37}\text{Ar}(n, p)^{37}\text{Cl}$  reactions occur in nucleosynthesis networks related to the weak s-process [1]. For the calculation of the corresponding stellar reaction rates, cross section data are needed for neutron energies from thermal up to a few hundred keV. In this respect, the reaction cross sections at thermal neutron energy are very valuable since they are frequently used as a normalization point for measurements in other energy regions and/or for the calculation of the  $1/v$  component in the Maxwellian averaged cross section [2]. So a precise knowledge of these cross sections is often required. Thermal neutron induced reaction cross sections can also give information about the presence of nearby resonances [3].

Neutron induced measurements on  $^{37}\text{Ar}$  are hampered by the fact that this isotope is not commercially available and furthermore has a relatively short half life of about 35 days. In the literature only one measurement on the reactions of interest is reported by Asghar et al. [4]. It was performed more than 20 years ago and the results have been obtained from only one single run. The  $^{37}\text{Ar}$  sample used contained  $1.98 \times 10^{13}$   $^{37}\text{Ar}$  atoms and the measurement resulted in cross section values of  $(1970 \pm 330)$  b for the  $(n_{\text{th}}, \alpha_0)$  and  $(69 \pm 14)$  b for the  $(n_{\text{th}}, p)$  reaction. With such large cross sections, the  $1/v$  component alone can dominate the Maxwellian averaged cross section. Therefore, the results reported by Asghar et al. [4] need to be verified and the uncertainties of these measurements should be reduced.

We could optimize the experimental conditions for a new measurement by combining the preparation of  $^{37}\text{Ar}$  samples yielding hundred times more atoms than in the case of Asghar et al. [4] with an accurate determination of the number of  $^{37}\text{Ar}$  atoms with a dedicated detector and a very intense and clean thermal neutron beam.

## 2 Sample preparation

One of the most crucial aspects for a precise cross section determination on  $^{37}\text{Ar}$  is the preparation and the characterization of the sample. A detailed description of the whole procedure is given in [5].

All samples were produced at the 30 MeV cyclotron at Louvain-la-Neuve, Belgium. The accelerated protons hit a NaCl target. The  $^{37}\text{Ar}$  atoms, created via the  $^{37}\text{Cl}(p,n)^{37}\text{Ar}$  reaction, were ionized ( $2^+$  or  $1^+$ ) and afterwards implanted in a  $20\ \mu\text{m}$  thin Al foil. Samples containing up to  $2\times 10^{15}$   $^{37}\text{Ar}$  atoms were produced corresponding to about 120 ng of  $^{37}\text{Ar}$  in the layer.

The number of  $^{37}\text{Ar}$  atoms was determined at the Institute for Reference Materials and Measurements in Geel, Belgium, by detecting the 2.62 keV KX rays of  $^{37}\text{Cl}$ , which is created by the pure electron capture decay of  $^{37}\text{Ar}$ . For this purpose a gas flow proportional detector was used.

For the present measurement four samples were used, containing  $10^{14}$ ,  $7.8\times 10^{14}$ ,  $1.4\times 10^{15}$  and  $2\times 10^{15}$   $^{37}\text{Ar}$  atoms, respectively, at the beginning of the measurements. The uncertainty of these values is 7% and mainly due to the uncertainty of some decay constants as explained in [5].

### 3 Experimental technique

All measurements were performed at the High Flux Reactor at the Institute Laue-Langevin (ILL) in Grenoble, France. The experimental setup was placed at the end of the 87 m curved neutron guide H22. Due to its slight curvature, the  $\gamma$ -ray flux was reduced by a factor  $10^6$ . The ratio of thermal to fast neutrons was  $10^6$ . The thermal neutron flux at the sample position was measured to be  $5\times 10^8\ \text{n}/\text{cm}^2\text{s}$ . A schematical top view of the experiment is depicted in Fig. 1.

The neutron beam entered the vacuum chamber through a thin Al window. The sample was mounted at  $30^\circ$  with respect to the neutron beam axis. This geometry ensured that the whole sample surface was irradiated by thermal neutrons. Surface barrier detectors with suited thicknesses were mounted outside the neutron beam. Their energy calibration was done by means of the  $^{10}\text{B}(n_{\text{th}},\alpha)^7\text{Li}$  and  $^6\text{Li}(n_{\text{th}},\alpha)\text{t}$  reactions.

All measurements were normalized via the well known  $^{235}\text{U}(n_{\text{th}},f)$  reaction cross section, using the value of  $(584.25\pm 1.10)\ \text{b}$  reported in the ENDF/B-VI data file. This neutron flux calibration was performed strictly maintaining the experimental geometry.

### 4 Measurements

The level scheme drawn in Fig. 2 illustrates the possible reactions. Since the

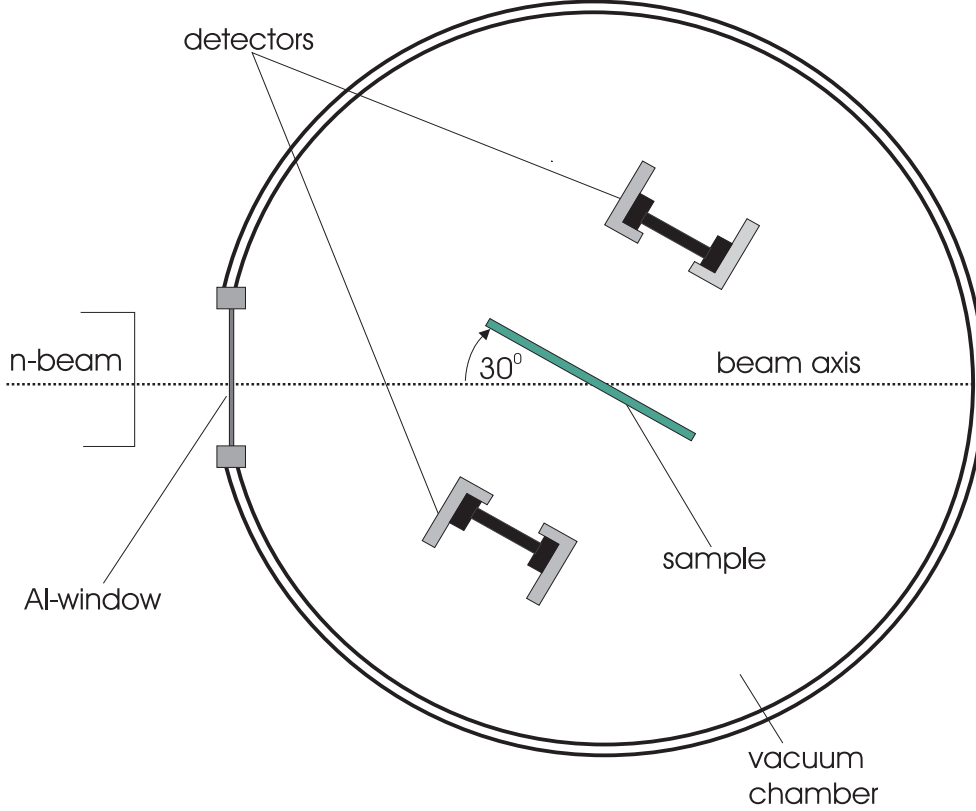


Fig. 1. Top view of the experimental setup at the ILL.

ground state of  $^{37}\text{Ar}$  is  $J^\pi=3/2^+$ , only  $1^+$  and  $2^+$  levels of the compound nucleus  $^{38}\text{Ar}$  will be populated during thermal neutron capture.

For the  $(n_{\text{th}},\alpha)$  reaction the  $1^+$  compound nucleus spin is ruled out, because  $\alpha$  emission from a  $1^+$  state to the  $0^+$  ground state of  $^{34}\text{S}$  is parity forbidden for initial  $s$ -waves. Most likely  $d$ -wave  $\alpha$  particles emitted from the  $2^+$  state of  $^{38}\text{Ar}$  will determine the  $(n_{\text{th}},\alpha_0)$  cross section. The  $(n_{\text{th}},\alpha_1)$  transition to the first excited state of  $^{34}\text{S}$  having a spin/parity assignment of  $2^+$  is allowed, where the corresponding  $\alpha$  particles have an energy of 2.239 MeV. Furthermore,  $(n_{\text{th}},\gamma\alpha)$  transitions are also possible in principle.

In the case of the  $(n_{\text{th}},p)$  reaction,  $s$ -wave protons may be emitted from the  $1^+$  as well as from the  $2^+$  state to the  $3/2^+$  ground state of  $^{37}\text{Cl}$ . The  $Q$ -values and corresponding particle energies are obtained using the masses from [6]:

$$\begin{aligned}
 Q_p &= 1.596 \text{ MeV} \text{ corresponding to } E_p = 1.554 \text{ MeV}, \\
 Q_{\alpha_0} &= 4.630 \text{ MeV} \text{ corresponding to } E_{\alpha_0} = 4.143 \text{ MeV} \text{ and} \\
 Q_{\alpha_1} &= 2.502 \text{ MeV} \text{ corresponding to } E_{\alpha_1} = 2.239 \text{ MeV}.
 \end{aligned}$$

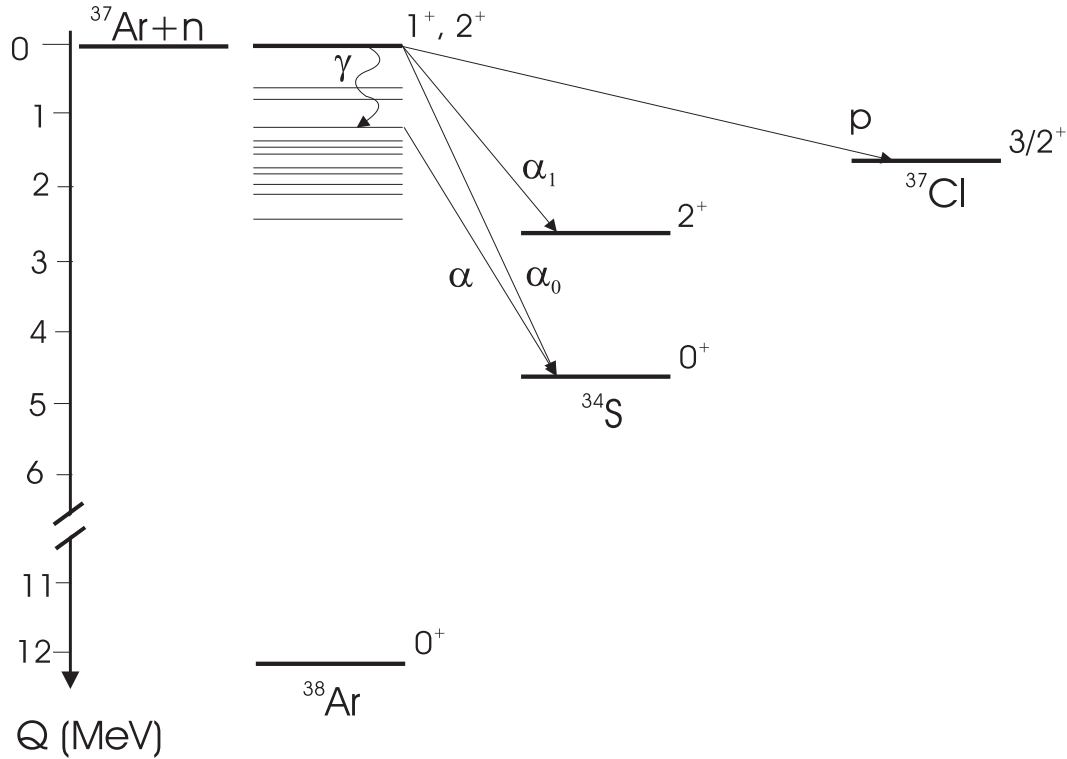


Fig. 2. Level scheme of the  $^{37}\text{Ar}(n_{\text{th}},\alpha)^{34}\text{S}$  and  $^{37}\text{Ar}(n_{\text{th}},p)^{37}\text{Cl}$  reactions.

#### 4.1 The reaction $^{37}\text{Ar}(n_{\text{th}},\alpha)^{34}\text{S}$

The choice of the detector characteristics is always a compromise between high energy resolution (thick detector) and low background (thin detector). The  $\alpha_0$  particles have a fairly high energy of 4.143 MeV, so the  $^{37}\text{Ar}(n_{\text{th}},\alpha_0)^{34}\text{S}$  reaction cross section could be measured by using a surface barrier detector with a thickness of 100  $\mu\text{m}$  and a resolution of 20 keV. Three measuring cycles were performed with three different samples starting with the thinnest one.

A significant improvement concerning statistics and signal-to-background ratio was reached with thicker samples. For the sample containing  $1.4 \times 10^{15}$   $^{37}\text{Ar}$  atoms the  $\alpha_0$  counting rate reached more than 5700 counts per hour. In Fig. 3 a typical spectrum of the  $^{37}\text{Ar}(n_{\text{th}},\alpha_0)^{34}\text{S}$  reaction is shown using this sample. The other peaks occurring at lower energy correspond to the  $\alpha$  and  $^7\text{Li}$  lines of the  $^{10}\text{B}(n_{\text{th}},\alpha)^7\text{Li}$  reactions for  $^{10}\text{B}$  impurities in the sample and the small peak at about 2.7 MeV is due to the tritons produced in the  $^6\text{Li}(n_{\text{th}},\alpha)t$  reaction. The shoulder at about 1.55 MeV is due to the protons emitted in the  $^{37}\text{Ar}(n_{\text{th}},p)^{37}\text{Cl}$  reaction.

For the  $^{37}\text{Ar}(n_{\text{th}},\alpha_1)$  particles, a much lower counting rate was expected, so the background conditions were more critical. Hence, a 25  $\mu\text{m}$  thick detector (resolution 60 keV) was used for this experiment. In Fig. 4 the result of 1100 h

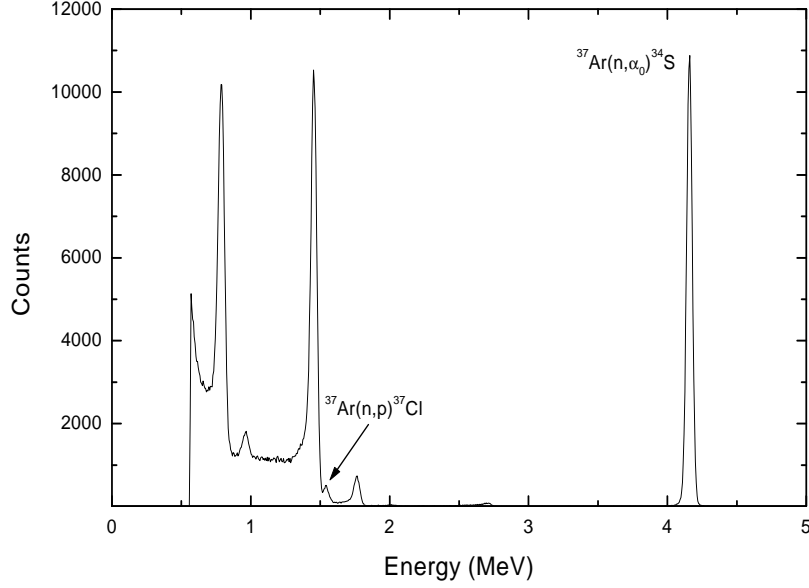


Fig. 3. Typical spectrum of the  $^{37}\text{Ar}(n_{\text{th}},\alpha_0)^{34}\text{S}$  reaction obtained with the sample containing  $1.4\times 10^{15}$   $^{37}\text{Ar}$  atoms using a  $25\ \mu\text{m}$  detector.

of data taking is shown. Two different samples containing respectively  $5\times 10^{14}$  and  $2\times 10^{15}$   $^{37}\text{Ar}$  atoms were used during this measurement.

#### 4.2 The reaction $^{37}\text{Ar}(n_{\text{th}},\gamma\alpha)^{34}\text{S}$

These measurements were also performed with the sample containing  $2\times 10^{15}$   $^{37}\text{Ar}$  atoms, using the  $25\ \mu\text{m}$  thick detector with an energy resolution of 60 keV. In this way, good background conditions could be realized down to about 2 MeV. The background in the  $(n,\gamma\alpha)$  region was determined during measurements with the reactor stopped and also with the reactor in operation and the sample rotated over  $180^\circ$ . The  $^{37}\text{Ar}(n_{\text{th}},\gamma\alpha)^{34}\text{S}$  spectrum in the region between the  $\alpha_0$  and  $\alpha_1$  peaks can also be seen in Fig. 4.

#### 4.3 The reaction $^{37}\text{Ar}(n_{\text{th}},p)^{37}\text{Cl}$

The problem of detecting the  $(n_{\text{th}},p)$  reaction becomes evident by looking at Fig. 3. The 1.554 MeV protons are almost completely hidden by the  $\alpha_0$ 's and  $\alpha_1$ 's induced in  $^{10}\text{B}$  impurities in the layer. Therefore, the setup used for the  $(n,\alpha)$  measurements was not suited for the determination of the  $(n,p)$  reaction.

In order to determine the  $^{37}\text{Ar}(n_{\text{th}},p)^{37}\text{Cl}$  reaction cross section, a mylar foil (chemical composition:  $\text{C}_{10}\text{H}_8\text{O}_4$ , density  $1.397\ \text{g}/\text{cm}^3$ ) with a thickness of  $5\ \mu\text{m}$  was put in front of the detector. Table 1 gives an overview of the energy

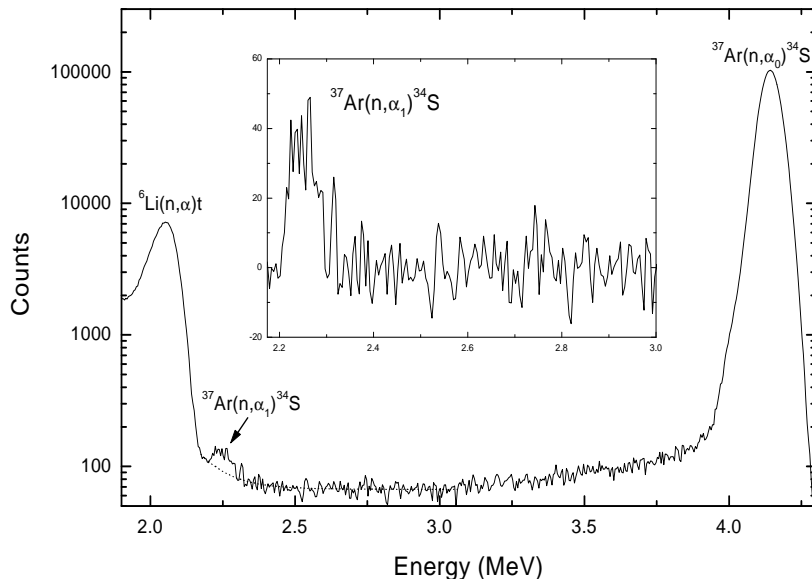


Fig. 4. Spectrum of the  $^{37}\text{Ar}(n_{\text{th}},\alpha_1)^{34}\text{S}$  and  $^{37}\text{Ar}(n_{\text{th}},\gamma\alpha)^{34}\text{S}$  reactions obtained with the sample containing  $2 \times 10^{15}$   $^{37}\text{Ar}$ -atoms and a  $25 \mu\text{m}$  detector. In the insert the region of the  $\alpha_1$ -transition corrected with a semi-empirical backgroundfit, is magnified.

loss in  $5 \mu\text{m}$  of mylar of the main particles considered, showing that 1.554 MeV protons will only lose about 0.12 MeV of their energy while the  $\alpha$ 's of  $^{10}\text{B}$  are almost stopped (calculated by using the FORTRAN code TRIM (TRansport of Ions in Matter [7])). Therefore, the proton peak should emerge from the huge background caused by  $^{10}\text{B}$  impurities.

Table 1

Overview of the energy loss of several particles in  $5 \mu\text{m}$  mylar.

Particle	Initial energy (MeV)	Energy loss (MeV)	Final energy (MeV)
p ( $^{37}\text{Ar}$ )	1.554	0.120	1.434
$\alpha$ ( $^{37}\text{Ar}$ )	4.143	0.650	3.493
$\alpha_0$ ( $^{10}\text{B}$ )	1.789	1.100	0.689
$\alpha_1$ ( $^{10}\text{B}$ )	1.483	1.200	0.283
$\alpha$ ( $^6\text{Li}$ )	2.007	1.000	1.007
t ( $^6\text{Li}$ )	2.727	0.220	2.507

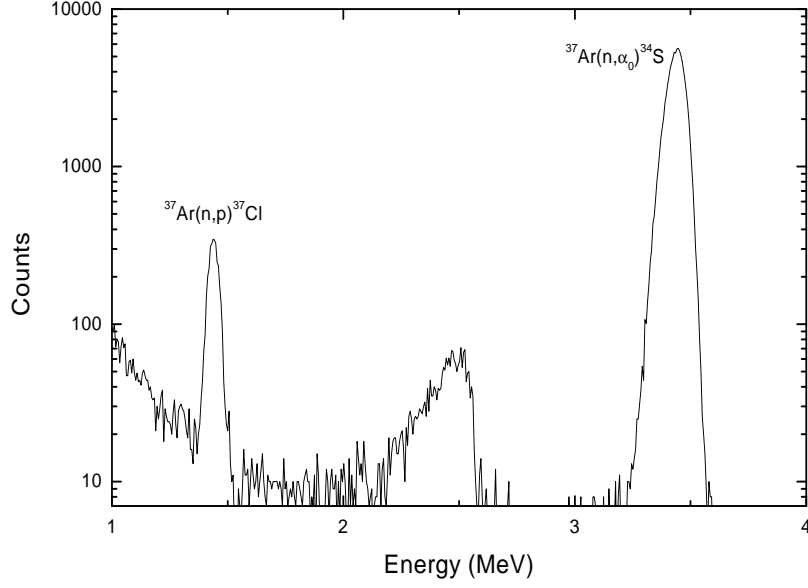


Fig. 5. Spectrum of the  $^{37}\text{Ar}(n,p)^{37}\text{Cl}$  reaction obtained with the sample containing  $1.4 \times 10^{15}$   $^{37}\text{Ar}$  atoms using a  $100 \mu\text{m}$  detector with  $5 \mu\text{m}$  of mylar in front.

The first measurement was again performed with the sample containing  $10^{14}$   $^{37}\text{Ar}$  atoms using a  $30 \mu\text{m}$  thick detector (energy resolution of 55 keV) in order to have a better signal-to-background ratio. We performed a similar measurement with a thicker  $^{37}\text{Ar}$  sample ( $1.4 \times 10^{15}$   $^{37}\text{Ar}$  atoms), this time using a  $100 \mu\text{m}$  thick detector with an energy resolution of 30 keV. Fig. 5 shows the result of a 16 hour measurement under these conditions. The count rate reached 200 protons per hour and the background correction could easily be done because the proton peak was situated at the end of the low energy noise. The  $^{37}\text{Ar}(n,p)^{37}\text{Cl}$  cross section was determined relative to the particles detected in the same measurement.

## 5 Results and discussion

### 5.1 The reaction $^{37}\text{Ar}(n_{th},\alpha)^{34}\text{S}$

The  $^{37}\text{Ar}(n_{th},\alpha)^{34}\text{S}$  reaction cross section value was determined relative to the  $^{235}\text{U}(n_{th},f)$  reaction using following formula:

$$\sigma_{\alpha} = \left( \frac{N_{\text{U}}}{N_{\text{Ar}}} \right) \left( \frac{C_{\alpha}}{C_{\text{f}}} \right) \left( \frac{g(T)_{\text{U}}}{g(T)_{\text{Ar}}} \right) \sigma_{\text{U}} \quad (1)$$

where  $N_{\text{U}}$  and  $N_{\text{Ar}}$  are the number of atoms/cm<sup>2</sup> of the  $^{235}\text{U}$  and the  $^{37}\text{Ar}$  samples,  $C_{\alpha}$  and  $C_{\text{f}}$  the counting rates of the  $^{37}\text{Ar}(n_{th},\alpha)^{34}\text{S}$  and  $^{235}\text{U}(n_{th},f)$



reactions,  $g(T)_{\text{Ar}}$  and  $g(T)_{\text{U}}$  the corresponding Westcott factors and  $\sigma_{\text{U}}$  the  $^{235}\text{U}(n_{\text{th}},f)$  reference cross section. A detailed derivation of this formula is given in [8], where also a value  $g(T)_{\text{U}} = 0.995 \pm 0.002$  is reported. Since the  $^{37}\text{Ar}(n_{\text{th}},\alpha_0)^{34}\text{S}$  cross section follows a  $1/v$  shape below 100 eV [9],  $g(T)_{\text{Ar}} = 1$  is adopted.

Due to the short half-life of  $^{37}\text{Ar}$ , the number of  $^{37}\text{Ar}$  atoms present in the sample had to be calculated for each run. The homogeneity of our samples was checked by mounting collimators in front of the sample.

The following  $(n_{\text{th}},\alpha_0)$  cross section values were obtained with the three samples used: 1055 b ( $10^{14}$  at.), 1085 b ( $7.8 \times 10^{14}$  at.) and 1070 b ( $1.4 \times 10^{15}$  at.). This illustrates the reproducibility of the measurements. Averaging over all measurements results in a value of  $(1070 \pm 80)$  b for the  $^{37}\text{Ar}(n_{\text{th}},\alpha)^{34}\text{S}$  reaction cross section. The error quoted includes all uncertainties, the main contribution arising from the uncertainty on the  $^{37}\text{Ar}$  atoms in the layer. This value is almost a factor of two lower than the one published by Asghar et al. [4].

The  $^{37}\text{Ar}(n_{\text{th}},\alpha_1)^{34}\text{S}$  cross section was determined relative to the  $^{37}\text{Ar}(n_{\text{th}},\alpha_0)^{34}\text{S}$  counts recorded in the same experiment. This yielded a  $\sigma(n_{\text{th}},\alpha_0)/\sigma(n_{\text{th}},\alpha_1)$  ratio of  $(3500 \pm 850)$ , the error being mainly due to the small number of events and to the background correction. With  $\sigma(n_{\text{th}},\alpha_0) = (1070 \pm 80)$  b this leads to a  $^{37}\text{Ar}(n_{\text{th}},\alpha_1)^{34}\text{S}$  cross section of  $(310 \pm 100)$  mb. This large ratio can be understood by a simple model calculation. Since the excitation energy of the compound nucleus  $^{38}\text{Ar}$  is 10.3 MeV, the reactions are overwhelmingly dominated by compound nuclear processes. For low energies the transmission functions of the compound nucleus are equal to the penetration probabilities  $P_\ell(E)$ , which can be written as [10]:

$$P_\ell(E) = \exp(-2\pi\eta) \quad \text{for } \ell = 0 \quad (2)$$

$$P_\ell(E) = P_0(E) \exp \left[ -2\ell(\ell + 1) \left( \frac{\hbar^2}{2\mu Z_1 Z_2 e^2 R_n} \right)^{\frac{1}{2}} \right] \quad \text{for } \ell \neq 0$$

with  $\eta = Z_1 Z_2 e^2 / (\hbar v)$  the Sommerfeld parameter and  $\ell$  the orbital angular momentum quantum number in the exit channel.  $Z_1$  and  $Z_2$  denote the integral charges of the interacting nuclei with a relative velocity  $v$  and a reduced mass  $\mu$ . The range of the nuclear force for the interacting nuclei is given by  $R_n = R_0(A_1^{1/3} + A_2^{1/3})$ .

Since the Coulomb barrier in the exit channels of the reaction is about 10 MeV and thus much higher than the corresponding energies of the interacting particles, we can use Eq. 2 to determine the penetration probabilities in the exit channels. The transition  $^{37}\text{Ar}(n_{\text{th}},\alpha_1)^{34}\text{S}$  to the first excited state is suppressed considerably more through the Coulomb barrier in the exit channel than the

$^{37}\text{Ar}(n_{\text{th}},\alpha_0)^{34}\text{S}$  transition to the ground state, because of the lower  $Q$ -value. The additional hindrance through the centrifugal barrier in the exit channel for the ground-state transition with  $\ell = 2$  compared to the transition to the first excited state with  $\ell = 0$  is much smaller than the dependence on the Coulomb barrier. Based on Eq. 2, we calculated a cross section ratio  $\sigma(n_{\text{th}},\alpha_0)/\sigma(n_{\text{th}},\alpha_1) = 4200$  that is in agreement with the experimental results.

### 5.2 The reaction $^{37}\text{Ar}(n_{\text{th}},\gamma\alpha)^{34}\text{S}$

The  $^{37}\text{Ar}(n_{\text{th}},\gamma\alpha)^{34}\text{S}$  cross section was determined in the region between the  $^{37}\text{Ar}(n_{\text{th}},\alpha_0)^{34}\text{S}$  and  $^{37}\text{Ar}(n_{\text{th}},\alpha_1)^{34}\text{S}$  lines. After a correction for the background and the low energy tailing from the  $\alpha_0$  peak, the counting rate in that region was integrated and the cross section was determined relative to the  $^{37}\text{Ar}(n_{\text{th}},\alpha_0)^{34}\text{S}$  counting rate. This yielded an estimation of  $(9 \pm 3)$  b for the  $^{37}\text{Ar}(n_{\text{th}},\gamma\alpha)^{34}\text{S}$  cross section.

### 5.3 The reaction $^{37}\text{Ar}(n_{\text{th}},p)^{37}\text{Cl}$

The  $^{37}\text{Ar}(n_{\text{th}},p)^{37}\text{Cl}$  reaction cross section was determined relative to the  $^{37}\text{Ar}(n_{\text{th}},\alpha_0)^{34}\text{S}$  counting rate obtained in the same measurement. The measurement with the thinnest  $^{37}\text{Ar}$  sample resulted in a  $\sigma_\alpha/\sigma_p$  ratio of  $(27.2 \pm 2.6)$ . The large uncertainty quoted is due to the limited statistics accumulated with this sample. A great improvement was realized by using a thicker  $^{37}\text{Ar}$  sample. The counting rate for the  $(n_{\text{th}},\alpha_0)$  and  $(n_{\text{th}},p)$  reactions was  $(92434 \pm 991)$  and  $(3178 \pm 87)$  counts, respectively, resulting in a ratio of  $(29.1 \pm 0.9)$ . So the total uncertainty of the ratio decreased to less than 3%. These results agree with the ratio of  $(28.5 \pm 2.7)$  obtained by Asghar et al. [4], which indicates that the origin of the discrepancy between both measurements lies in the determination of the number of  $^{37}\text{Ar}$  atoms in the sample or in the neutron flux determination.

The weighted average of our two measurements yields a value of  $(37 \pm 4)$  b for the  $^{37}\text{Ar}(n_{\text{th}},p)^{37}\text{Cl}$  cross section, which again is about two times smaller than the value of  $(69 \pm 14)$  b reported by Asghar et al. .

## 6 Conclusion

In the present work the  $^{37}\text{Ar}(n_{\text{th}},\alpha_0)^{34}\text{S}$  reaction cross section was determined using three different samples. The results were perfectly reproducible and led

to an average value of  $(1070 \pm 80)$  b, which is about two times smaller than the results reported by Asghar et al. [4]. Also a weak  $^{37}\text{Ar}(n_{\text{th}},\alpha_1)^{34}\text{S}$  transition with a cross section of  $(310 \pm 100)$  mb was observed. For the  $^{37}\text{Ar}(n_{\text{th}},p)^{37}\text{Cl}$  cross section we obtained a value of  $(37 \pm 4)$  b. Also  $^{37}\text{Ar}(n_{\text{th}},\gamma\alpha)^{34}\text{S}$  transitions were clearly observed resulting in an estimation of  $(9 \pm 3)$  b for the cross section.

## References

- [1] H. Schatz, S. Jaag, G. Linker, R. Steininger, F. Käppeler, P. E. Koehler, S. M. Graff and M. Wiescher, *Phys. Rev.* **C51** (1995) 379.
- [2] Z. Bao and F. Käppeler, *Atomic Data and Nuclear Data Tables* **36** (1987) 411.
- [3] N. Balabanov, V. Vtyurin, Y. Gledenov and J. Popov, *Sov. J. Part. Nucl.* **21** (1990) 131.
- [4] M. Asghar, A. Emsallem, E. Hagberg, B. Jonson and P. Tidemand-Petersson, *Z. Phys.* **A288** (1978) 45.
- [5] C. Wagemans, M. Loiselet, R. Bieber, B. Denecke, D. Reher and P. Geltenbort, *Nucl. Instr. and Meth.* **A397** (1997) 22.
- [6] G. Audi and A.H. Wapstra, *Nucl. Phys.* **A595** (1995) 409.
- [7] J.F. Ziegler and J.M. Manoyan, *Nucl. Instr. and Meth.* **B35** (1988) 215.
- [8] C. Wagemans, P. Schillebeeckx and J. P. Bocquet, *Nucl. Sci. Eng.* **101** (1989) 293.
- [9] C. Wagemans, G. Goeminne, R. Bieber, J. Wagemans, M. Gaelens, M. Loiselet, B. Denecke, P. Geltenbort and F. Kolen, *Proc. Int. Conf. on Nuclei in the Cosmos V, Volos (GR)* (1998) in print.
- [10] C. E. Rolfs and W. S. Rodney, *Cauldrons in the Cosmos*, The University of Chicago Press: Chicago, 1988.